Computers and Electronics in Agriculture 199 (2022) 107170

Contents lists available at ScienceDirect

Computers and Electronics in Agriculture

journal homepage: www.elsevier.com/locate/compag

Prediction of total volatile basic nitrogen (TVB-N) and 2-thiobarbituric acid (TBA) of smoked chicken thighs using computer vision during storage at 4 °C

Bo Wang [a,1], Hongyao Yang [a,1], Cong Yang [a], Fenggui Lu [a], Xiaodan Wang [b], Dengyong Liu [a,c,*]

[a] College of Food Science and Technology, Bohai University, Jinzhou 121013, China
[b] College of Food Science and Engineering, Jilin University, Changchun 130062, China
[c] Jiangsu Collaborative Innovation Center of Meat Production and Processing, Quality and Safety Control, Nanjing 210095, China

A R T I C L E I N F O

Keywords:
Smoked chicken thigh
Computer vision
Freshness
TVB-N
TBA

A B S T R A C T

As the traditional indicators of freshness measurement of meat products, TVB-N and TBA have the disadvantage of time-consuming, labor-intensive and destructive to the sample. The objective of this study was to investigate the possibility of computer vision techniques to visualize the variation of TVB-N and TBA during the storage of smoked chicken thighs. In this study, freshness indicators (TVB-N and TBA) and images of smoked chicken thighs were obtained simultaneously every 3 days during storage at 4 °C. Then, the RGB color space was converted to HSI and $L^*a^*b^*$ color spaces by color conversion algorithm, and the color parameters (RGB, HSI and $L^*a^*b^*$) were correlated with TVB-N and TBA, respectively, for establishing multiple regression models. Finally, visualization maps of the spoilage were established by applying the multiple regression model to each pixel in the image. The results showed that the multiple linear regression models of TBA and TVB-N based on the color parameters L^*, a^*, I, S and R were well correlated ($R^2 = 0.993$ for TBA and $R^2 = 0.970$ for TVB-N). Distribution maps of TBA and TVB-N changed color gradually from blue to red during storage, respectively. In conclusion, this study demonstrated that distribution maps can be employed as a rapid, objective, and non-destructive method to predict the TBA and TVB-N values of smoked chicken thighs during storage.

1. Introduction

Smoked chicken thighs, as one of the traditional foods of smoking meat, have the characteristics of unique smoky aroma (Zhang et al., 2021a) and appealing smoky color (Wang et al., 2021a,b; Zhang et al., 2021b), which are popular among numerous customers. However, protein dehydration, denaturation, degradation, and lipid oxidation may occur during storage or industrial processing due to the rich nutritional properties of smoked chicken thighs, which will affect its freshness (Lan et al., 2016). Therefore, freshness, as one of the most important factors in evaluating the quality and safety of meat, is highly correlated with the sales and consumption of smoked chicken thighs.

In general, there are two main methods to assess the freshness of food products: subjective measurement and objective measurement. Sensory analysis, as a subjective measurement method, is conducted by the assessors and involves the use of eyesight, touch, and olfaction (Karpinska-Tymoszczyk, 2014). Objective measurement methods include physical methods such as texture (Dang et al., 2021), color (Lan et al., 2016) and electronic nose (Bekhit et al., 2021); chemical methods such TBA content (Karpinska-Tymoszczyk, 2014) and TVB-N content (Liu et al., 2020; Lan et al., 2016); biochemical methods such as trimethylamine (TMA), biogenic amine formation (Bekhit et al., 2021) and microbiological methods such as flat colony counting method (Wang et al., 2020; Shange et al., 2019). These objective analytical methods are more accurate than sensory analysis and play a critical part in the current methods of freshness evaluation. However, a considerable amount of time and energy is required to carry out these traditional determination methods, and it can also be destructive to the sample (Shi et al., 2018). Meanwhile, the analytical reagents used in the experiments are potentially harmful to the laboratory staff and the environment

* Corresponding author at: College of Food Science and Technology, Bohai University, No. 19 Keji Road, Songshan District, Jinzhou 121013, Liaoning Province, China.
E-mail address: jz_dyliu@126.com (D. Liu).

[1] Bo Wang and Hongyao Yang contributes equally to this work.

https://doi.org/10.1016/j.compag.2022.107170
Received 12 October 2021; Received in revised form 12 June 2022; Accepted 22 June 2022
Available online 27 June 2022

(Dallinger et al., 2020). Therefore, developing an objective, rapid and non-destructive method to evaluate the freshness of smoked chicken thighs would be significant to the smoked chicken industry due to its potential economic effect.

Computer vision has been applied as a fast and non-destructive method to evaluate food quality by analyzing color changes (Saldaña et al., 2014). It is also a critical technique for evaluating food freshness (Shi et al., 2018). It has the advantages of efficiency, objectivity, consistency and reliability. Recently, there are more and more researches using computer vision evaluates the quality of chicken (Taheri-Garavand et al., 2019), fish (Dowlati et al., 2013) and pork (Saldaña et al., 2014) by color features. However, meat spoilage is a complicated and dynamic process due to the tissue enzymes and microorganisms. It is common for meat degradation that accompanies simultaneous changes in internal properties (chemical composition) and external properties (color, texture and odor) (Shi et al., 2018; Lan et al., 2016). According to You et al. (2020), lipid oxidation and protein decomposition during storage will accelerate myoglobin oxidation and eventually led to the color change of meat. By establishing the multiple linear regression model. Zhang et al. (2019) determined that color was highly correlated with the freshness index of chilled lamb. The freshness of red mullet was evaluated using the image processing tool associated with chemical and sensory analysis by Tappi et al. (2017).

However, traditional methods for predicting the content of components can only obtain the average value of the measured parameters and cannot provide their space distribution. Meanwhile, due to the fact that the location distribution of each pixel in the sample image was spatial, it provided the possibility to map the spatial distribution of different physicochemical components. For example, Cheng et al. (2016) performed pseudo-color visualization of the established partial least squares regression (PLSR) model with the biogenic amine index corresponding to each pixel in the hyperspectral image to achieve the mapping of pork biogenic amine index on the spatial image. Shi et al. (2018) proposed that the freshness of tilapia could be represented visually as a distribution map based on images acquired by computer vision. Torres et al. (2021) established a distribution map of almond fatty acids through the established partial least squares (PLS) regression model and hyperspectral images. Meanwhile, Wang et al. (2021a,b) achieved not only the prediction of tea polyphenol content in each pixel of the tea spectral image by transferring the filtered optimal prediction model to each pixel of the hyperspectral image, but also visualized the spatial distribution of tea polyphenols in tea samples by the established distribution map. However, there were no studies reported to obtain the spatial distribution of TBA and TVB-N during the storage of smoked chicken thighs directly by distribution maps.

The objective of this study was to investigate the feasibility of distribution maps as a rapid and non-destructive method for predicting the freshness of smoked chicken thighs based on computer vision technology. It provides a reference for future research on the use of computer vision to predict other freshness parameters and may also provide a way for the meat industry to achieve real-time monitoring of changes in the quality of smoked chicken products.

1.1. Materials and chemicals

In order to benchmark the actual production of the company and reduce the effect of freezing on the quality of raw meat (Qi et al., 2021), 390 (160 ± 10 g) chicken thighs were provided by Liaoning Goubanzi Food Co., Ltd (Liaoning, China) with a freezing time of less than two weeks. The unpeeled chicken thighs were about 5.5 cm in diameter. All the chicken thighs were transferred to the Lab at Bohai University in a cooling box at 2–4 °C. Sucrose was purchased from Nanjing Ganjuyuan Sugar Industry Co., Ltd. (Nanjing, China). All spices were purchased from a supermarket located in Jinzhou, Liaoning Province, China. Neutral filter paper, packaging bag (18 × 25 × 0.016 cm), anhydrous alcohol, methyl red and all other chemical reagents of analytical grade were supplied by Jinzhou National Pharmaceutical Co., Ltd. (Jinzhou, China).

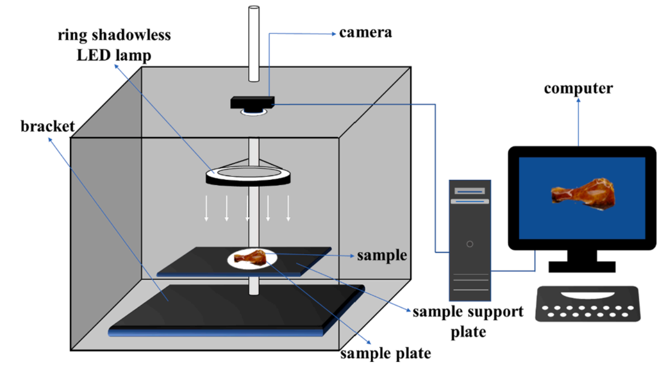

Fig. 1. Structure diagram of smoked chicken thighs image acquisition device.

1.2. Preparation of smoked chicken thighs

The preparation of sugar-smoked chicken thighs was referred to the method described by Wang et al. (2021a,b). The technology of sugar smoking was as follows: Chicken thighs were thawed under running water at room temperature (25 ± 5 °C) and were blanched. Boiled chicken thighs in brine for 10 min, and then simmered for 90 min. The recipe for the spices of the brine was prepared according to the method of Wang et al. (2021a,b). Then, remove the chicken thighs from the brine and chill it to room temperature (25 ± 5 °C).

Sucrose (350 g) was added and began to produce smoke when the temperature of the sugar heating plate in the sugar fumigation furnace (YXDT1/1, Hebei Xiaojin Machinery Manufacturing Co., Ltd., Hebei, China) with a length, width and height of 152 × 130 × 260 cm, respectively, increased to 330 °C. When the furnace temperature reached 100 °C, the chicken thighs were hung in the sugar fumigation furnace and sugar smoking for 8 mins. The sucrose amount used in each batch was equal. When the temperature cooled to 15 ± 5 °C, the oil stains were removed from the surface of the chicken thighs. Afterwards, each sugar-smoked chicken thigh was packed in vacuum (DZ-600, Jinda, China) tagged with the date and sequence number with storage in a refrigerator at 4 °C for 36 days. Finally, collect chicken thighs images and determine the TVB-N value and TBA value every three days for 36 days. A total of 13 groups of sample images and corresponding TVB-N value and TBA value were obtained.

1.3. Image acquisition system

The image acquisition system is shown in Fig. 1. The image collection system was composed of an imaging chamber (Pangniu Technology Co., Ltd., Shenzhen, China), a bracket (ES400300, LOTS, Dongguan, China), a digital camera (EOS 600D, Canon, Tokyo, Japan), a computer (Y7000P, Lenovo, Beijing, China), a ring LED shadowless light (HPR200, LOTS, Dongguan, China) for image processing. The imaging chamber was 50 cm in length, width and height. A ring shadowless LED lamp (power of 15.2 W and color temperature of 6500 Kelvin) with an external diameter of 21.5 cm and an internal diameter of 17 cm was fixed in the middle of the top of the imaging chamber. This ring shadowless LED lamp is a planar light source, which can maximally reduce the reflection problem in the process of taking images. The bracket was placed inside the imaging chamber. The sample support plate was fixed to the bracket and can be moved vertically to adjust the distance between the sample and the camera, which minimizes the reflection and color deviation caused by the unsuitable light distance. The camera lens was placed in a round hole of 6 cm, which was created in the center of the top of the imaging chamber.

1.4. Image analysis

The Python program was applied to obtain and analyze the color information of the sugar-smoked chicken thighs in three steps. First, images were acquired by a digital camera for the smoked chicken thighs. Secondly, the R, G and B information of the image was obtained by computer vision. Finally, the RGB values were transformed into HSI and $L^*a^*b^*$ values by image analysis algorithms.

1.4.1. Image acquisition and preprocessing

As the purpose of this study was to achieve nondestructive detection of spoilage degree of smoked chicken thighs, thus images were collected from vacuum-packed smoked chicken thighs. The digital camera was positioned vertically above the sample plate with the lens at a distance of 40 cm from the sample surface. This distance not only obtains a satisfactory image, but also minimizes the reflection problem caused by vacuum packaging. A total of 30 smoked chicken thighs were selected randomly from the refrigerator every 3 days to obtain pictures. The sample was flipped 90° after acquiring one image, and four images were acquired in total for one sample. The external humidity of the sample was wiped before image acquisition. It was RGB color images that were collected in the experiment. The resolution of these images was 5184 × 3456 pixels and the format was PNG. To better display the effect of image preprocessing and obtain the local image from the whole smoked chicken thighs, the resolution of the image was reduced to 384 × 384 pixels. After the image was rotated, flipped and stretched randomly, the three new images were generated. It changed the position and orientation of the original image without changed the image properties. The number of sample images was increased and the accuracy of the test results was enhanced by preprocessing the images.

1.4.2. Convert RGB to $L^*a^*b^*$ and HSI

It was common that the color spaces RGB (red, green, blue), HSI (hue, saturation and intensity) and $L^*a^*b^*$ (lightness, redness and yellowness) were applied in food classification (Hashim et al., 2011). As a linear color space, RGB color spaces can be acquired rapidly through computer vision systems. Color differences on a uniform scale cannot be represented by RGB space only (Cheng et al., 2001). Thus, it does not easily distinguish the similarity of two colors using the RGB values. The HSI color space can help overcome the speed limitations related to color-based computer vision compared to the RGB color space (Gunasekaran, 1996). In contrast to the RGB and HSI color spaces, the $L^*a^*b^*$ color space contains a broader color gamut, which indicates that $L^*a^*b^*$ can exhibit a broader range of colors (Yam and Papadakis, 2004). The RGB color space was converted to HSI and $L^*a^*b^*$ color spaces to better describe the color information of smoked chicken thighs (Łuszczkiewicz-Piątek, 2014).

1.4.2.1. Convert RGB into $L^*a^*b^*$. As described by León et al. (2006), the RGB color space was converted to $L^*a^*b^*$ color space in two steps.

Firstly, RGB values were converted to XYZ values.

$$X = 0.412453R + 0.3578G + 0.180423B \quad (1)$$

$$Y = 0.212671R + 0.71516G + 0.072169B \quad (2)$$

$$Z = 0.019334R + 0.119193G + 0.950227B \quad (3)$$

Second step, convert XYZ values to $L^*a^*b^*$ values.

$$L^* = 116f(Y/Y_n)\text{-}16 \quad (4)$$

$$a^* = 500[f(X/X_n)\text{-}f(Y/Y_n)] \quad (5)$$

$$b^* = 200[f(Y/Y_n)\text{-}f(Z/Z_n)] \quad (6)$$

$$f(t) = \begin{cases} \sqrt[3]{t} & \text{if } t > \left(\frac{6}{29}\right)^3 \\ \frac{1}{3}\left(\frac{29}{6}\right)^2 t + \frac{4}{29} & \text{if } t \le \left(\frac{6}{29}\right)^3 \end{cases} \quad (7)$$

where $X_n = 95.047$, $Y_n = 100.0$, $Z_n = 108.883$, t refers to $f(X/X_n)$, $f(Y/Y_n)$, $f(Z/Z_n)$.

The L^* a^* b^* values of each storage period were compared with day 0 to determine the change in color difference (ΔE) of smoked chicken thighs in the whole storage period.

$$\Delta E = \sqrt{(L_0^*\text{-}L_i^*)^2 + (a_0^*\text{-}a_i^*)^2 + (b_0^*\text{-}b_i^*)^2} \quad (8)$$

where ΔE represents the absolute color difference; L_0^*, a_0^*, b_0^* represents the color parameters on day 0; L_i^*, a_i^*, bi^* represents the color parameters on day i.

1.4.2.2. Convert RGB into HSI. The RGB values were transformed into HSI values according to the method of Rotaru et al. (2008).

$$I = \frac{R + G + B}{3} \quad (9)$$

$$S = 1 - \frac{3}{R + G + B} \times \min(R, G, B) \quad (10)$$

$$H = \cos^{-1}\left(\frac{0.5 \times [(R\text{-}G) + (R\text{-}B)]}{\sqrt{(R\text{-}G)^2 + (R\text{-}B)(G\text{-}B)}}\right) \quad (11)$$

1.5. Total volatile basic nitrogen (TVB-N)

TVB-N was assessed by the semi-micro Kjeldahl method used by Hu et al. (2013). The analytical conditions were as follows: The method was as follows: distilled water (100 mL) was added into the minced sample (10 g) and then stirred with an electronic stirrer (30 min) (Allegra 64R, Thunder Magnetic Instrument Co., Ltd., Shanghai, China). Then, after centrifugation at 5500 r for 15 min (USA.JB-2A, Thunder Magnetic Instrument Co., Ltd., Shanghai, China), the mixture was filtered through ordinary filter paper, and the filtration was repeated twice to collect the permeate. Afterwards, 5 mL of the resulting filtrate and 5 mL of MgO suspension (10 g/L) were added into the tube, with 10 mL of boric acid (20 g/L) as the acceptor and then distilled using a Kjeldahl Apparatus (K9840, Haineng Scientific Instrument Co., Ltd, Shandong, China). The boric acid absorbent solution was titrated by 0.01 mol/L hydrochloric acid (HCl).

1.6. Thiobarbituric acid value (TBA)

The TBA values were measured by the approach proposed by Lan et al. (2016). The minced sample (10 g) was mixed with 20% trichloroacetic acid (TCA) (w/v) solution (25 mL) and homogenized at 10,000 rpm for 30 s (FW-200, Zhongxingweiye Instruments Co., Ltd., Beijing, China). The supernatant was filtered twice after centrifugation at 5500 rpm for 15 min at 4 °C (Allegra 64R, Thunder Magnetic Instrument Co., Ltd., Shanghai, China). The filtrate (2 mL) and 0.02 mol/L TBA (2 mL) were mixed in a test tube and heated in a water bath at 80 °C for 20 min. Then, the solution was cooled 10 min in an ice bath. The absorbance of the sample was determined at 532 nm by using water as a blank (UV2550, Spectrum General Technology Co., Ltd., Beijing, China). A control sample was prepared and treated with the same procedure.

1.7. Establishment of the multiple linear regression model

Multiple linear regression modeling was a statistical technique that

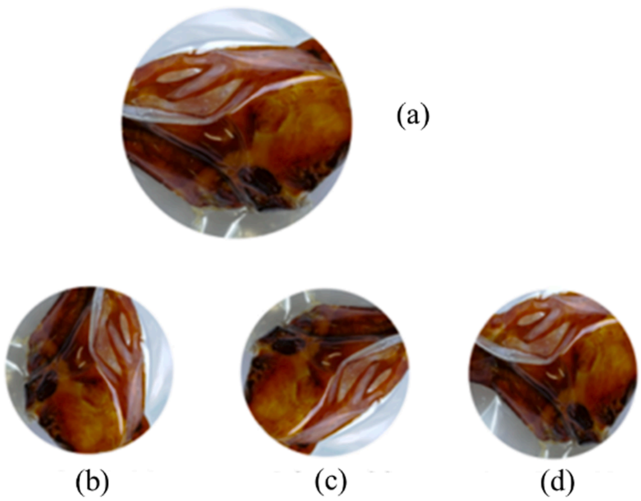

Fig. 2. Image pre-processing results of smoked chicken thighs. (a) Original image, (b) random rotation image, (c) random flip image, (d) stretch transformation image.

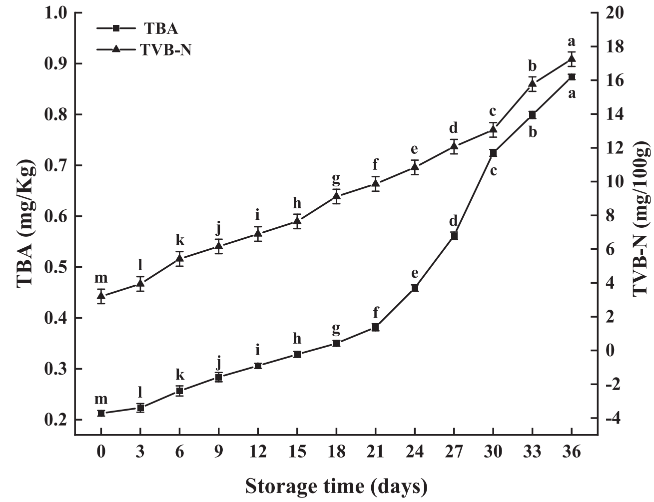

Fig. 3. Variation of TVB-N and TBA in smoked chicken thighs stored at 4 °C. Different letters indicated that there was significant difference ($p < 0.05$). Error bars indicated standard deviations.

was used to model the linear relationship between the independent variables (explanatory variables) and the dependent variables (response variables). Therefore, the L^*, a^*, S, I, and R were used as independent variables while the TBA and TVB-N were used as dependent variables, respectively, while in order to compare the influence of changes in the independent variables on the model coefficients of determination, three corresponding multiple linear regression models were established separately. The first group took the color parameters R, a^*, I and S as the independent variable. The color parameters R, L^*, a^*, S and R, S, I, L^*, a^* were used as independent variables for the second and third groups, respectively. Variance inflation factor (VIF) was utilized as a measurement to evaluate the multi-collinearity among the independent variables in the multiple regression model (Liu et al., 2008). When the VIF values of the respective variables showed less than 10, it indicated that there was no significant multi-collinearity and the regression model was well fitted (Yoon and Lee, 2021).

1.8. Distribution maps for TVB-N and TBA values

The deterioration degree of smoked chicken thighs cannot be determined directly by color change during storage at 4 °C. Therefore, developing a fast and intuitive method to evaluate the freshness and quality of smoked chicken thighs was necessary. The effective approach to obtaining the freshness of smoked chicken thighs during storage was visualizing TVB-N and TBA values. There were corresponding color data for each pixel of the image. Hence, the freshness metrics of each pixel can be predicted through multiplying each pixel of the image by the regression coefficient of the model and visualized it according to a linear color scale (Cheng et al., 2016). In this research, the best models will be applied to convert each pixel of the image into the corresponding color separately and finally to generate the distribution maps of TBA and TVB-N. The variation of the color in the distribution map from blue to red indicated the TVB-N and TBA values increased from low to high. Changes in TBA and TVB-N in smoked chicken thigh samples can be easily estimated by observing the colors in the distribution map.

1.9. Statistical analysis

The python programming language in the OpenCV platform (Open-Source Computer Vision Library) was utilized to carry out the image processing algorithms, multiple regression algorithms, and visualization procedures, and then uploaded to the device. Experimental data on color, TBA, TVB-N were statistically analyzed using IBM SPSS Statistics 26 (SPSS Inc., Chicago, IL, USA) software to analyze variance (ANOVA). All the results were expressed as mean ± standard deviation (M ± SD). Multiple comparisons of means were established by Duncan's multiple range test. Differences were significantly at $p < 0.05$. Figures were plotted by applying Origin 2021 software (OriginLab Corp, Northampton, USA). The R^2 was employed to estimate the fit degree of the model.

2. Results and discussion

2.1. Image acquisition results

120 images were collected for each storage time, and 1560 images were collected for 13 storage times. Image preprocessing results showed in Fig. 2. There were 480 pictures in each storage time (including 120 original images, 120 random rotation images, 120 random flip images and 120 stretch transformation images) and 6240 pictures in the whole storage time.

2.2. Chemical indicators analysis

2.2.1. Total volatile basic nitrogen content (TVB-N)

The variation of TVB-N content in smoked chicken thighs from day 0 to day 36 was shown in Fig. 3. There was a significant increase of TVB-N values from 3.2 mg/100 g to 17.25 mg/100 g with the extension of storage time ($p < 0.05$). TVB-N value was the ammonia and amine basic nitrogen-containing substances produced by meat or meat products via the action of enzymes and spoilage microorganisms (Bekhit et al., 2021; Lan et al., 2016). Therefore, the increase in TVB-N values of smoked chicken thighs during storage was predictable. As shown by Khulal et al. (2016), microbial spoilage and deterioration of meat and meat products reached unacceptable when the TVB-N values reached 15 mg N/100 g. Smoked chicken thighs exceeded 15 mg N/100 g at day 30, longer than the reported cooked chicken. Balamatsia et al. (2007) found that the growth of aerobic spoilage bacteria (Pseudomonas and Yeast) could be inhibited in poultry products during the refrigeration process, which reduced the rate of protein decomposition and significantly extended the shelf life. Meanwhile, study by Cyprian et al. (2015) showed that the dehydration effect of the smoking process, the antimicrobial action of the smoke components and the high temperature function of the hot smoke also resulted in a significant reduction of the microbial content at the beginning of storage, which increased the storage period of smoked chicken thighs. Besides, the antimicrobial components in the smoke will

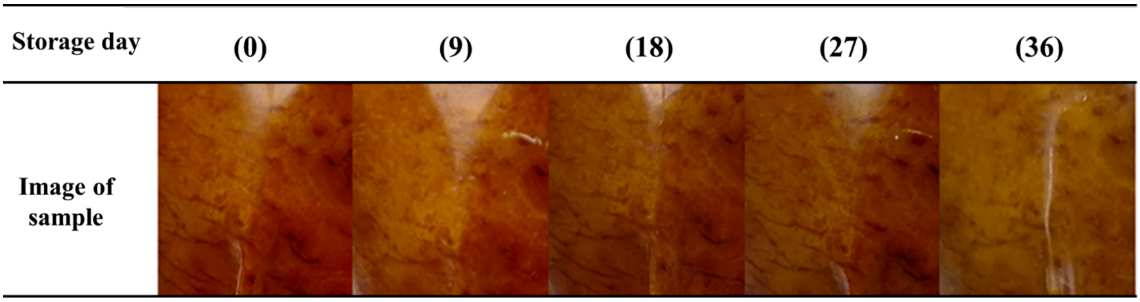

Fig. 4. Typical images of color changes at days 0, 9, 18, 27, and 36 of smoked chicken thighs stored at 4 °C.

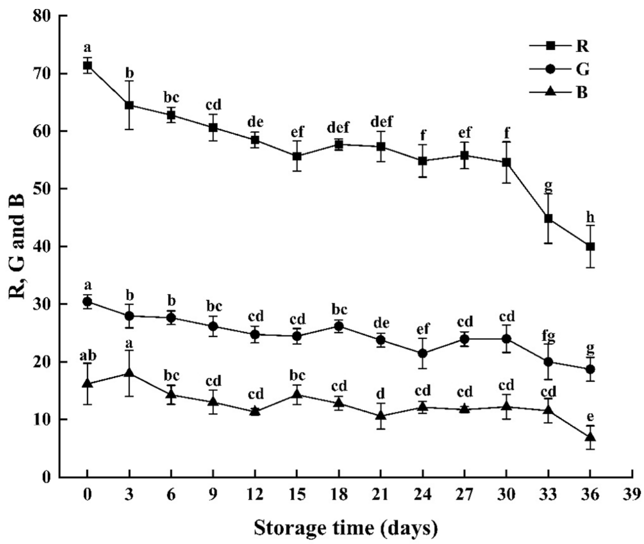

Fig. 5. Variation of color parameters (R, G, B) of smoked chicken thighs during storage at 4 °C. Different letters indicated significant differences ($p < 0.05$). Error bars indicated standard deviations. R = indicates red; G = indicates green; B = indicates blue.

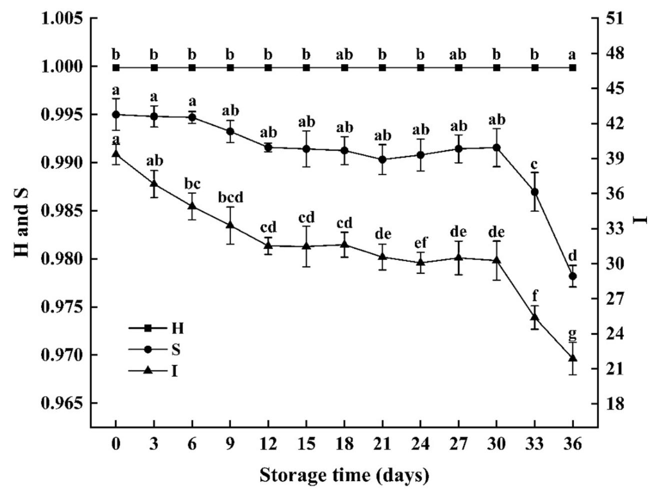

Fig. 6. Variation of color parameters (H, S, I) of smoked chicken thighs during storage at 4 °C. Different letters indicated significant differences ($p < 0.05$). Error bars indicated standard deviations. H = indicates hue; S = indicates saturation; I = indicates intensity.

continuously inhibition the growth of microorganisms during the storage. However, in this study, smoked chicken thighs (Fig. 3) had a lower initial TVB-N value (3.2 mg N/100 g) than the cooked chicken meat (5.74 mg N/100 g) (Khulal et al.et al., 2016). It was probably related to the dehydration, antibacterial and antioxidant activity that resulted from smoking (Leroi and Joffraud, 2000).

2.2.2. Thiobarbituric acid content (TBA)

The variation of TBA values for the smoked chicken thighs was shown in Fig. 3. The TBA values of the smoked chicken thighs increased significantly ($p < 0.05$) from 0.21 mg/kg (day 0) to 0.87 mg/kg (day 36) during storage. Similar findings were achieved by Al-Hijazeen et al. (2018). TBA values were widely reported to determine the content of malondialdehyde (MDA), a fat oxidation product (Liu et al., 2020). As demonstrated by Karpinska-Tymoszczyk (2014), and Georgantelis et al. (2007), the rancid flavor was detected in meat products with MDA content higher than 0.6 mg/kg. The present results showed that smoked chicken thighs were up to the rancid level after 29 days of storage. It was possibly due to the antioxidant properties of the phenolics produced by the smoking process, which prevented the polyunsaturated fatty acids from the oxidation and even enhanced the oxidative stability (Yu et al., 2018). The research in Dang et al. (2021) indicated that vacuum withdraws the air from the package and will reduce some of the ongoing oxidation processes. The initial TBA value of smoked chicken thighs in this study were lower than smoked chicken breast (1.21 mg/100 g) by Gettinger et al. (2017). This result agrees with Al-Hijazeen et al. (2018), who found that the TBA value of chicken breast was higher than those of the chicken thigh meat.

2.3. Computer vision imaging of smoked chicken thighs

The typical images for smoked chicken thighs at days 0, 9, 18, 27 and 36 were displayed in Fig. 4. The color of the smoked chicken thighs gradually becomes yellowish from the initial bright yellow–brown color with the increase of storage time. Lipid hydroperoxides were produced by lipid oxidation during the storage of smoked chicken thighs (Valous et al., 2009). Subsequently, low molecular weight carbonyl and alcohol compounds were generated through the decomposition of hydroperoxides, which led to the quality changes of smoked chicken thighs by influencing color, flavor, odor and texture (Shange et al., 2019; Liu et al., 2019). Overall, the dynamics of organic compounds, proteolysis and lipid oxidation were associated with changes in the freshness of smoked chicken thighs.

*2.4. Change of RGB, L*a*b* and HSI*

Fig. 5 showed the change in the RGB color space of smoked chicken thighs stored **under 4 °C for 36 days. The values of R, G and B decreased with the increase of storage days. According to Fig. 5, the R value decreased significantly from 71.40 to 40.01 ($p < 0.05$), the G value decreased significantly from 30.45 to 18.72 ($p < 0.05$), as well as the B value also decreased significantly from 16.19 to 6.88 ($p < 0.05$) during storage. It can be seen from Fig. 5 that the R value and G value were higher than the B value. It was attributed to the dominant color (yellow)

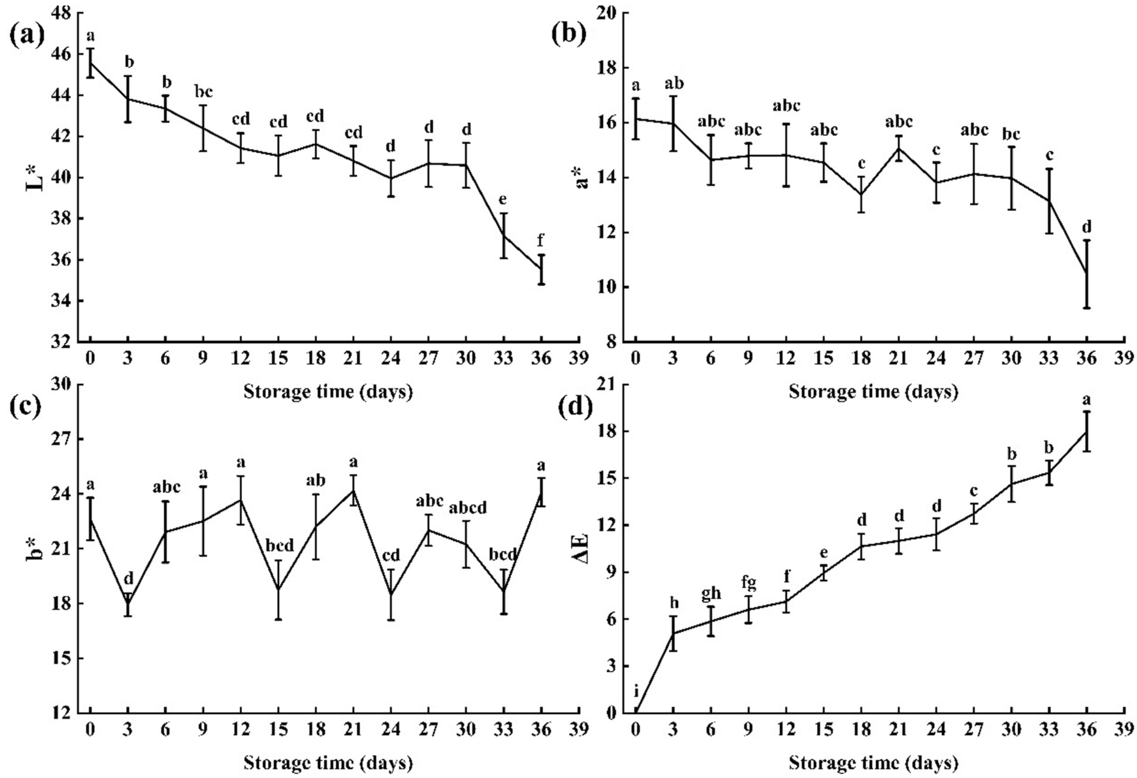

Fig. 7. Variation of color parameters (L* a* b*) of smoked chicken thighs during storage at 4 °C for (a) L*, (b) a*, (c) b* and (d) ΔE. Different letters indicated significant differences ($p < 0.05$). Error bars indicated standard deviations. L* = indicates lightness; a* = indicates redness; b* = indicates yellownes.

of smoked chicken thighs was consisted of high red and green, with low or minimal content of blue (Hashim et al., 2011). R value decreased with the increase of storage time, which demonstrated that red decreased. According to Shi et al. (2018), the decrease of red color was affected by meat texture, water content, pigments, and activators enzyme that play a role in the formation and degradation of meat color. It can be seen from Fig. 5 that the G and B values decreased, but the variations were smaller compared to the R values. Therefore, the G and B values were not effective indexes to evaluate the freshness, while the R value can be used as an effective indicator to evaluate the freshness of smoked chicken thighs.

The result of HSI of all samples is shown in Fig. 6. It can be noticed that the S value decreased significantly with the extension of storage days. The initial S value of smoked chicken thighs was 0.9950 and decreased to 0.9782 at the end of storage days. The S component represented that the saturation changed at varying illumination levels (Shi et al., 2018), which meant that the color saturation of smoked chicken thighs decreased gradually as the storage time increase. As shown in Fig. 6, the I value decreased significantly from 30.35 to 21.87 ($p < 0.05$). The decrease of I value was consistent with the decrease of color brightness during storage because I value also represents the brightness of the image (Dhandra et al., 2006). The H value was about 1° (red) throughout the storage time ($p > 0.05$). Vieira et al. (2009) found that the use of vacuum packaging during the storage of chicken meat may increase the stability of metmyoglobin and consequently the stable Hue (H value) during the storage period. Hence, the H value was not an available color parameter to evaluate changes in freshness during storage.

Fig. 7 showed the result of the $L^*a^*b^*$ color of smoked chicken thighs stored under 4 °C for 36 days. Generally, all results showed a decrease in L^* values and a^* value, whereas the b^* value fluctuated by storage time. This agreed with the results of Yang and Chen (1993), and Lan et al. (2016) stated that a^* value and L^* values of chicken meat decreased significantly and b^* value did not change significantly after storage. According to Fig. 7(a), Fig. 7(b) and Fig. 7(c), the L^* value decreased significantly from 40.56 to 30.52 ($p < 0.05$), the a^* value decreased significantly from 16.13 to 10.47 ($p < 0.05$), whereas the b^* value showed a fluctuation trend during storage (17.940–24.184). Shi et al. (2018) indicated that the reduction of the brightness was probably due to the reduction of the moisture content during storage. Adrah et al. (2021) indicated that the b^* values of chicken meat treated with quercetin for antioxidant coating were fluctuating during storage compared to the control group without antioxidant coating treatment, similar to the results of this study. It suggested that the fluctuation of b^* values in this study was most probably caused by the formation of antioxidant coating on the surface of chicken thighs by the phenolic antioxidants produced during the smoking process. The decrease in a^* was probably due to the release of iron from the hemoglobin molecule by the oxidation of denatured globulin and the oxidative cleavage of hemoglobin pigments (Dang et al., 2021). The ΔE values increased from 0 on day 0 to 17.99 on day 36 ($p < 0.05$) (Fig. 7(d)) due to the rapid change of color in the smoked chicken thighs during storage. A similar phenomenon was reported for tilapia by Shi et al. (2018). Therefore, the b^* value was not an effective index for evaluating the freshness of smoked chicken thighs, while the L^* value and a^* value have a changing trend, which can be used as an effective index to evaluate the freshness of smoked chicken thighs.

Overall, L^*, a^*, S, I, R have a high correlation with the color of smoked chicken thighs during storage, which is suitable for describing the color change.

2.5. Multiple regression model results

As a parameter that evaluated the linear correlation between the independent variables, when the VIF was higher than 10, it indicated that there was significant multi-collinearity between the independent variables (Liu et al., 2008). The results of multiple linearity detection for the independent variables in the multiple regression model were shown

Table 1
Multi-collinearity results of the independent variables.

Statistics/Parameters	Tolerance analysis (1 - R^2)	VIF
a *	0.599	1.670
I	0.113	8.841
L	0.149	6.693
S	0.325	3.073
R	0.111	9.011

Table 2
Regression models for freshness prediction between indicators and color parameters of smoked chicken thighs during storage at 4 °C.

Index	Model	R^2	p-Value
Y_{TBA}	Y1 = 79.388 + 0.172a* + 0.231I − 81.405S − 0.14R	0.947	0.009
	Y2= − 150.109–0.307a* − 0.884L* + 178.289S + 0.255R	0.976	0.002
	Y3= − 78.209–0.167a* + 100.299S + 0.156I + 0.138R − 0.759L*	0.993	0.002
D_{TVB-N}	D1 = 683.082 + 2.228a* + 1.781I − 684.647S − 1.464R	0.956	0.000
	D2= − 1417.07–2.119a* − 8.369L* + 1697.18S + 2.063R	0.968	0.000
	D3= − 921.468–1.195a* + 1164.772S + 1.165I + 1.292R − 7.728L*	0.970	0.000

Y (dependent variable): TVB-N value, D (dependent variable): TBA value.

in Table 1, and the VIF values of the independent variables L, *a**, S, I, and R ranged from 1.670 to 9.011, indicating that there was no significant correlation between the independent variables (Yoon and Lee, 2021). From the Table 2, it can be found that the *p*-values corresponding to the F-values in the multiple linear regression model were all lower than 0.05, which indicated that the color parameters of the model had a significant effect on the TBA and TVB-N values. Y represented the multiple linear regression equation of TBA and D represented the multiple linear regression equation of TVB-N. The R ^{2} of the Y1, Y2 and Y3 models were 0.947, 0.976 and 0.993, respectively. The Y3 model showed the best performance ($R^2 = 0.993$) by further comparing the results of the three models. Meanwhile, the R^2 of the D1, D2 and D3 models were 0.956, 0.968 and 0.970, respectively. Compared with D1 and D2 models, the D3 model showed better performance ($R^2 = 0.970$). It can be found from the results that the differences in the independent variables I and L caused the coefficients of determination of the models Y1 and D1 were lower than those of Y2 and D2, which indicated that the color parameters I and L had a greater influence on the coefficients of determination of the models. Meanwhile, compared with models of Y1, Y2, D1, and D2, the coefficients of determination of models Y3 and D3 were also increased due to the addition of both independent variables I and L, reaching 0.993 and 0.970, respectively. Therefore, each pixel of TBA and TVB-N value were predicted by the best models of Y3 and D3, respectively.

2.6. Distribution map results

The distribution maps for TBA and TVB-N at days 0, 9, 18, 27 and 36 were shown in Fig. 8 and Fig. 9, respectively. It indicated that the different TBA and TVB-N values were displayed by the different colors of the distribution maps. The pixels with different color parameters represented the corresponding TVB-N and TBA values in the distribution map, respectively (Cheng et al., 2016). Fig. 8 displayed the distribution maps of the TVB-N values of smoked chicken thighs at different storage periods with color scales at the bottom. It is noticeable that there was a tendency for the color change from blue to red with the increase of TVB-N values, reflecting the accumulation of TVB-N and the decrease of freshness. For example, Fig. 8(A) showed a uniform distribution of blue and green with a low TVB-N value of 3.2 mg/100 g, implying that the smoked chicken thighs were fresh. Fig. 8(E) showed mostly the red color distribution of TVB-N values with a high TVB-N value of 17.25 mg/100

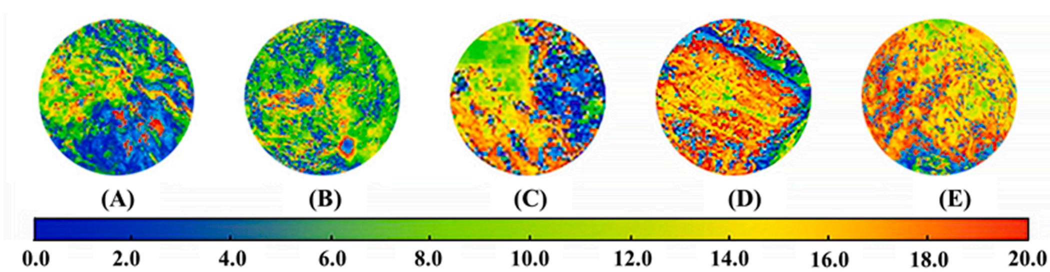

Fig. 8. Examples of distribution maps of smoked chicken thighs at different TVB-N values (Linear color scale, from blue to red, was used to visualize the TVB-N values of each pixel, in which the TVB-N with low values were displayed in blue and those with high values in red). (A) TVB-N = 3.2 mg/kg, storage for 0 days; (B) TVB-N = 6.16 mg/kg, storage for 9 days; (C) TVB-N = 9.12 mg/kg, storage for 18 days; (D) TVB-N = 12.07 mg/kg, storage for 27 days; (D) TVB-N = 17.25 mg/kg, storage for 36 days. (For interpretation of the references to color in this figure legend, the reader is referred to the web version of this article.)

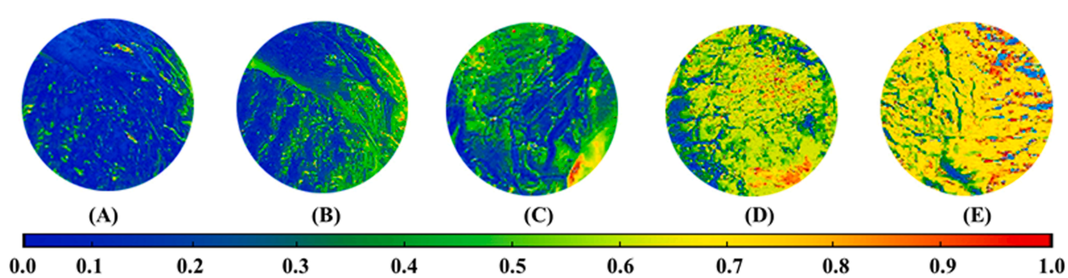

Fig. 9. Examples of distribution maps of smoked chicken thighs at different TBA values (Linear color scale, from blue to red, was used to visualize the TBA values of each pixel, in which the TBA with low values were displayed in blue and those with high values in red). (A) TBA = 0.21 mg/kg, storage for 0 days; (B) TBA = 0.28 mg/kg, storage for 9 days; (C) TBA = 0.35 mg/kg, storage for 18 days; (D) TBA = 0.56 mg/kg, storage for 27 days; (D) TBA = 0.87 mg/kg, storage for 36 days. (For interpretation of the references to color in this figure legend, the reader is referred to the web version of this article.)

g, indicated that a significant level of spoilage occurred. Fig. 9 showed the distribution maps of TBA for samples at different storage periods (0, 9, 18, 27, and 36 days, respectively). The color in the distribution map of sample storage at 0 days exhibited mostly blue (TBA was 0.21 mg /kg), which indicated that there was almost no malondialdehyde in the smoked chicken thighs samples (Fig. 9 (E)). According to Fig. 9(E), the distribution map of TBA values was almost yellow, and TBA values were up to 0.87 mg/kg, indicated that a significant level of spoilage happened. As the storage time increasing, the density of blue color became less, and the yellow color appeared more, demonstrated the increase of TBA content during storage. It was worth noting that the color densities in the distribution maps of TVB-N and TBA on day 18 showed a non-uniform, non-symmetric distribution (Fig. 8(C) and Fig. 9 (C)), which was similar to the findings of Zhenjie et al. (2015) and Cheng et al. (2016). It is probably attributed to the differences in the distribution of dominant microorganisms in the mid-storage period by differences in the oxygen content of different parts after vacuum packing (Balamatsia et al., 2006), which led to the different degradation rates of compounds. Therefore, the spoilage rates of different parts of smoked chicken thighs in the mid-storage period were different.

3. Conclusion

This study investigated the feasibility of a distribution map based on a computer vision system to predict the freshness of smoked chicken thighs during storage at 4 °C. Results displayed that the values of TVB-N and TBA increased with the increase of storage time. The R, G, B, S, I, L^*, a^* and ΔE values increased with the storage time, while there was no change in the H and b^* values. Multiple regression models of TVB-N and TBA based on color parameters (L^*, a^*, R, S, I) have the best performance with R^2 of 0.970 and 0.993, respectively. The color of the distribution maps for the TBA and TVB-N values changed from green to red, respectively, during the storage period. The research findings that the freshness of smoked chicken thighs can be predicted rapidly and non-destructively by distribution maps in an online manner. However, due to the differences in the process of sugar smoking and the selection of raw materials for different sugar-smoked products, the color of the sugar-smoked products after sugar smoking and the color change during the storage process will be different, which will have an impact on the final generated distribution map. Therefore, more research must be conducted to predict the freshness of other sugar-smoked products during storage in a stable and flexible way with distribution maps.

CRediT authorship contribution statement

Bo Wang: Conceptualization, Project administration, Software, Data curation. **Hongyao Yang:** Methodology, Writing – original draft, Formal analysis, Investigation. **Cong Yang:** Writing – review & editing. **Fenggui Lu:** Methodology, Investigation. **Xiaodan Wang:** Writing – review & editing. **Dengyong Liu:** Conceptualization, Funding acquisition, Supervision.

Declaration of Competing Interest

The authors declare that they have no known competing financial interests or personal relationships that could have appeared to influence the work reported in this paper.

Acknowledgements

This study was sponsored by the National Key R&D Program of China (grant numbers 2016YFD0401505) and the Liaoning Revitalization Talents Program (grant number XLYC1807100).

References

Adrah, K., Ananey-Obiri, D., Tahergorabi, R., 2021. Physicochemical Changes of Deep-Fat-Fried Chicken Drumsticks Treated with Quercetin-in-Edible Coating during Storage Time. Foods 10 (2), 467. https://doi.org/10.3390/foods10020467.

Al-Hijazeen, M., Mendonca, A., Lee, E.J., Ahn, D.U., 2018. Effect of oregano oil and tannic acid combinations on the quality and sensory characteristics of cooked chicken meat. Poult. Sci. 97 (2), 676–683. https://doi.org/10.3382/ps/pex285.

Balamatsia, C., Patsias, A., Kontominas, M., Savvaidis, I., 2007. Possible role of volatile amines as quality-indicating metabolites in modified atmosphere-packaged chicken fillets: Correlation with microbiological and sensory attributes. Food Chem. 104 (4), 1622–1628. https://doi.org/10.1016/j.foodchem.2007.03.013.

Balamatsia, C.C., Paleologos, E.K., Kontominas, M.G., Savvaidis, I.N., 2006. Correlation between microbial flora, sensory changes and biogenic amines formation in fresh chicken meat stored aerobically or under modified atmosphere packaging at 4 degrees C: possible role of biogenic amines as spoilage indicators. Antonie Van Leeuwenhoek 89 (1), 9–17. https://doi.org/10.1007/s10482-005-9003-4.

Bekhit, A.E.D.A., Holman, B.W.B., Giteru, S.G., Hopkins, D.L., 2021. Total volatile basic nitrogen (TVB-N) and its role in meat spoilage: A review. Trends Food Sci. Technol. 109, 280–302. https://doi.org/10.1016/J.TIFS.2021.01.006.

Cheng, H., Jiang, X., Sun, Y., Wang, J., 2001. Color image segmentation: advances and prospects. Pattern Recogn. 34 (12), 2259–2281. https://doi.org/10.1016/S0031-3203(00)00149-7.

Cheng, W., Sun, D., Cheng, J., 2016. Pork biogenic amine index (BAI) determination based on chemometric analysis of hyperspectral imaging data. LWT-Food Sci. Technol. 73, 13–19. https://doi.org/10.1016/j.lwt.2016.05.031.

Cyprian, O.O., Van Nguyen, M., Sveinsdottir, K., Jonsson, A., Tomasson, T., Thorkelsson, G., et al., 2015. Influence of smoking and packaging methods on lipid stability and microbial quality of Capelin (Mallotus villosus) and Sardine (Sardinella gibossa). Food Sci. Nutrition 3 (5), 404–414. https://doi.org/10.1002/fsn3.233.

Dallinger, D., Gutmann, B., Kappe, C.O., 2020. The concept of chemical generators: on-site on-demand production of hazardous reagents in continuous flow. Acc. Chem. Res. 53 (7), 1330–1341. https://doi.org/10.1021/acs.accounts.0c00199.

Dang, T.T., Rode, T.M., Skipnes, D., 2021. Independent and combined effects of high pressure, microwave, soluble gas stabilization, modified atmosphere and vacuum packaging on microbiological and physicochemical shelf life of precooked chicken breast slices. J. Food Eng. 292, e110352 https://doi.org/10.1016/j.jfoodeng.2020.110352.

Dhandra, B.V., Hegadi, R., Hangarge, M., Malemath, V.S., 2006. Analysis of abnormality in endoscopic images using combined HSI color space and watershed segmentation. In: International Conference on Pattern Recognition.

Dowlati, M., Mohtasebi, S.S., Omid, M., Razavi, S.H., Jamzad, M., Guardia, M., 2013. Freshness assessment of gilthead sea bream (Sparus aurata) by machine vision based on gill and eye color changes. J. Food Eng. 119 (2), 277–287. https://doi.org/10.1016/j.jfoodeng.2013.05.023.

Georgantelis, D., Blekas, G., Katikou, P., Ambrosiadis, I., Fletouris, D.J., 2007. Effect of rosemary extract, chitosan and alpha-tocopherol on lipid oxidation and colour stability during frozen storage of beef burgers. Meat Sci. 75 (2), 256–264. https://doi.org/10.1016/j.meatsci.2006.07.018.

Gettinger, S., Rizvi, N., Chow, L., Borghaei, H., Brahmer, J., Shepherd, F., et al., 2017. OA03.01 First-line nivolumab monotherapy and nivolumab plus ipilimumab in patients with advanced NSCLC: long-term outcomes from checkMate 012. J. Thoracic Oncol. 12 (1), 250–251. https://doi.org/10.1016/j.jtho.2016.11.238.

Gunasekaran, S., 1996. Computer vision technology for food quality assurance. Trends Food Sci. Technol. 7 (8), 245–256. https://doi.org/10.1016/0924-2244(96)10028-5.

Hashim, N., Janius, R.B., Baranyai, L., Rahman, R.A., Osman, A., Zude, M., 2011. Kinetic model for colour changes in bananas during the appearance of chilling injury symptoms. Food Bioprocess Technol. 5 (8), 2952–2963. https://doi.org/10.1007/s11947-011-0646-z.

Hu, S., Luo, Y., Cui, J., Lu, W., Wang, H., You, J., et al., 2013. Effect of silver carp (Hypophthalmichthys molitrix) muscle hydrolysates and fish skin hydrolysates on the quality of common carp (Cyprinus carpio) during 4 °C storage. Int. J. Food Sci. Technol. 48 (1), 187–194. https://doi.org/10.1111/j.1365-2621.2012.03176.x.

Karpinska-Tymoszczyk, M., 2014. The effect of antioxidants, packaging type and frozen storage time on the quality of cooked turkey meatballs. Food Chem. 148, 276–283. https://doi.org/10.1016/j.foodchem.2013.10.054.

Khulal, U., Zhao, J., Hu, W., Chen, Q., 2016. Nondestructive quantifying total volatile basic nitrogen (TVB-N) content in chicken using hyperspectral imaging (HSI) technique combined with different data dimension reduction algorithms. Food Chem. 197, 1191–1199. https://doi.org/10.1016/j.foodchem.2015.11.084.

Lan, Y., Shang, Y., Song, Y., Dong, Q., 2016. Changes in the quality of superchilled rabbit meat stored at different temperatures. Meat Sci. 117, 173–181. https://doi.org/10.1016/j.meatsci.2016.02.017.

León, K., Mery, D., Pedreschi, F., León, J., 2006. Color measurement in L * a * b * units from RGB digital images. Food Res. Int. 39 (10), 1084–1091. https://doi.org/10.1016/j.foodres.2006.03.006.

Leroi, F., Joffraud, J.J., 2000. Salt and smoke simultaneously affect chemical and sensory quality of cold-smoked salmon during 58 ℃ storage predicted using factorial design. J. Food Prot. 63 (9), 1222–1227. https://doi.org/10.4315/0362-028X-63.9.1222.

Liu, H., Ji, Z., Liu, X., Shi, C., Yang, X., 2020. Non-destructive determination of chemical and microbial spoilage indicators of beef for freshness evaluation using front-face synchronous fluorescence spectroscopy. Food Chem. 321, e126628 https://doi.org/10.1016/j.foodchem.2020.126628.

Liu, J., Li, Q., Dong, J., Chen, J., Gu, G., 2008. Multivariate Modeling of Aging in Bottled Lager Beer by Principal Component Analysis and Multiple Regression Methods. J. Agric. Food. Chem. 56 (16), 7012–7106. https://doi.org/10.1021/jf800879v.

Liu, Z., Zhong, Y., Hu, Y., Yuan, L., Luo, R., Chen, D., Wu, M., Huang, H., Li, Y., 2019. Fluorescence strategy for sensitive detection of adenosine triphosphate in terms of evaluating meat freshness. Food Chem. 270, 573–578. https://doi.org/10.1016/j.foodchem.2018.07.041.

Łuszczkiewicz-Piątek, M., 2014. Which color space should be chosen for robust color image retrieval based on mixture modeling. In: Image Processing and Communications Challenges.

Qi, J., Zhang, W.-W., Xu, Y., Xie, X.-F., Xiong, G.-Y., Xu, X.-L., Zhou, G.-H., Ye, M., 2021. Enhanced flavor strength of broth prepared from chicken following short-term frozen storage. Food Chem. 356, 129678. https://doi.org/10.1016/j.foodchem.2021.129678.

Rotaru, C., Graf, T., Zhang, J., 2008. Color image segmentation in HSI space for automotive applications. J. Real-Time Image Proc. 3 (4), 311–322. https://doi.org/10.1007/s11554-008-0078-9.

Saldaña, E., Siche, R., Castro, W., Huamán, R., Quevedo, R., 2014. Measurement parameter of color on yacon (Smallanthus sonchifolius) slices using a computer vision system. LWT - Food Sci. Technol. 59 (2), 1220–1226. https://doi.org/10.1016/j.lwt.2014.06.037.

Shange, N., Makasi, T., Gouws, P., Hoffman, L.C., 2019. Preservation of previously frozen black wildebeest meat (Connochaetes gnou) using oregano (Oreganum vulgare) essential oil. Meat Sci. 148, 88–95. https://doi.org/10.1016/j.meatsci.2018.10.012.

Shi, C., Qian, J., Han, S., Fan, B., Yang, X., Wu, X., 2018. Developing a machine vision system for simultaneous prediction of freshness indicators based on tilapia (Oreochromis niloticus) pupil and gill color during storage at 4 °C. Food Chem. 243, 134–140. https://doi.org/10.1016/j.foodchem.2017.09.047.

Taheri-Garavand, A., Fatahi, S., Shahbazi, F., Guardia, M.D.L., 2019. A nondestructive intelligent approach to real-time evaluation of chicken meat freshness based on computer vision technique. J. Food Process Eng 42 (4), e13039. https://doi.org/10.1111/jfpe.13039.

Tappi, S., Rocculi, P., Ciampa, A., Romani, S., Balestra, F., Capozzi, F., Dalla Rosa, M., 2017. Computer vision system (CVS): a powerful non-destructive technique for the assessment of red mullet (Mullus barbatus) freshness. Eur. Food Res. Technol. 243 (12), 2225–2233. https://doi.org/10.1007/s00217-017-2924-0.

Torres, I., Pérez-Marín, D., Vega-Castellote, M., Sánchez, M.-T., 2021. Mapping of fatty acids composition in shelled almonds analysed in bulk using a Hyperspectral Imaging system. LWT-Food Sci. Technol. 138, 110678. https://doi.org/10.1016/j.lwt.2020.110678.

Valous, N.A., Mendoza, F., Sun, D.W., Allen, P., 2009. Colour calibration of a laboratory computer vision system for quality evaluation of pre-sliced hams. Meat Sci. 81 (1), 132–141. https://doi.org/10.1016/j.meatsci.2008.07.009.

Vieira, C., Diaz, M.T., Martinez, B., Garcia-Cachan, M.D., 2009. Effect of frozen storage conditions (temperature and length of storage) on microbiological and sensory quality of rustic crossbred beef at different states of ageing. Meat Sci. 83 (3), 398–404. https://doi.org/10.1016/j.meatsci.2009.06.013.

Wang, B., Yang, H., Lu, F., Yu, F., Wang, X., Zou, Y., et al., 2021a. Establish Intelligent Detection System to Evaluate the Sugar Smoking of Chicken Thighs. Poult. Sci. 100 (11), e101447 https://doi.org/10.1016/j.psj.2021.

Wang, Y., Liu, Y., Chen, Y., Cui, Q., Li, L., Ning, J., Zhang, Z., 2021b. Spatial distribution of total polyphenols in multi-type of tea using near-infrared hyperspectral imaging. LWT 148, 111737. https://doi.org/10.1016/j.lwt.2021.111737.

Wang, Z., Shi, Y., Zhou, K., Zhou, H., Li, X., Li, C., Wang, Z., Xu, B., 2020. Effects of different thermal temperatures on the shelf life and microbial diversity of Dezhou-braised chicken. Food Res. Int. 136, 109471. https://doi.org/10.1016/j.foodres.2020.109471.

Yam, K.L., Papadakis, S.E., 2004. A simple digital imaging method for measuring and analyzing color of food surfaces. J. Food Eng. 61 (1), 137–142. https://doi.org/10.1016/S0260-8774(03)00195-X.

Yang, C.C., Chen, T.C., 1993. Effects of refrigerated storage, pH adjustment, and marinade on color of raw and microwave cooked chicken meat. Poult. Sci. 72 (2), 355–362. https://doi.org/10.3382/PS.0720355.

Yoon, S., Lee, W., 2021. Methodological analysis of bioclimatic variable selection in species distribution modeling with application to agricultural pests (Metcalfa pruinosa and Spodoptera litura). Comput. Electron. Agric. 190, e106430 https://doi.org/10.1016/j.compag.2021.106430.

You, Y., Her, J.Y., Shafel, T., Kang, T., Jun, S., 2020. Supercooling preservation on quality of beef steak. J. Food Eng. 274, e109840 https://doi.org/10.1016/j.jfoodeng.2019.109840.

Yu, L., Chai, M., Zeng, M., He, Z., Chen, J., 2018. Effect of lipid oxidation on the formation of N(epsilon)-carboxymethyl-lysine and N(epsilon)-carboxyethyl-lysine in Chinese-style sausage during storage. Food Chem., 269, 466-472. https://doi.org/10.1016/j.foodchem.2018.07.051.

Zhang, G., Huang, X., Fu, Z., Taha Jilani, M., Luo, H., Li, X., 2019. Correlation between physical properties and freshness of chilled mutton in China. J Food Process Preserv 43 (12). https://doi.org/10.1111/jfpp.v43.1210.1111/jfpp.14231.

Zhang, L., Hu, Y., Wang, Y., Kong, B., Chen, Q., 2021a. Evaluation of the flavour properties of cooked chicken drumsticks as affected by sugar smoking times using an electronic nose, electronic tongue, and HS-SPME/GC-MS. LWT 140, 110764. https://doi.org/10.1016/j.lwt.2020.110764.

Zhang, L., Wang, H., Xia, X., Xu, M., Kong, B., Liu, Q., 2021b. Comparative study on the formation of heterocyclic aromatic amines in different sugar smoking time. Food Control 124, e107905. https://doi.org/10.1016/J.FOODCONT.2021.107905.

Zhenjie, X., Da-Wen, S., Hongbin, P., Anguo, X., Zhong, H., Man, L., 2015. Non-destructive prediction of thiobarbituricacid reactive substances (TBARS) value for freshness evaluation of chicken meat using hyperspectral imaging. Food Chem. 179, 175–181. https://doi.org/10.1016/j.foodchem.2015.01.116.